Int J CARS (2006) 1:33–38
DOI 10.1007/s11548-006-0002-3

ORIGINAL ARTICLE

Shape discrimination of healthy and diseased cardiac ventricles using medial representation

Roland Pilgram · Rainer Schubert · Karl D. Fritscher · Ralf H. Zwick · Michael F. Schocke · Thomas Trieb · Otmar Pachinger

Published online: 24 February 2006

Abstract Our work aims at investigating the suitability of the medial representation method to model and analyze shape and shape differences between healthy and diseased hearts. For this experimental study, we use MRI short axis scans of 11 healthy volunteers (age: 50±10) and 5 patients (age: 57±11) with dilativ cardiomyopathy. Controlled semi-automated segmentation provides labels, which are used for the modeling process. To evaluate the model to image accuracy the similarity index (SI), the mean Euclidean distance (ED), and the Hausdorff distance (HD) are calculated. A very high SI (SI $>$ 0.9) for the ventricles is achieved. The mean ED is less than two times the voxel size (1.56 mm) and the HD values for both chambers are in the range of 4.8±3 mm. Applying extended principal component analysis (PCA) on all 16 subjects reveals the distribution of the individual shapes, where the first two PC cover more than 40%, and the first ten PC cover 95% of the shape space. The components show meaningful modes of variation, whereas the healthy and diseased hearts are clustered in the first two components. This preliminary result using the medial based approach promises to discriminate at least globally between healthy and diseased hearts.

R. Pilgram (✉) · R. Schubert · K.D. Fritscher
Institute for Biomedical Image Analysis (IBIA),
University for Health Sciences,
Medical Informatics and Technology Tyrol (UMIT), Tyrol, Austria
E-mail: roland.pilgram@umit.at
Tel.: +43-508648-3825
Fax: +43-508648-3830

R.H. Zwick · O. Pachinger
Department of Cardiology,
University Hospital of Innsbruck, Innsbruck, Austria

M.F. Schocke · T. Trieb
Department of Radiology I,
University Hospital of Innsbruck, Innsbruck, Austria

Keywords Heart modeling · Cardiomyopathy · Statistical shape analysis · Medial representation · Multiple objects

Introduction

Analysis of shape begins to emerge as a useful method of medical image computing with the potential to improve the accuracy of medical diagnosis as well as the understanding of processes behind growth and disease. Therefore, a variety of object representations have been suggested for 3D shape analysis over the last years.

In the field of modeling and analyzing the complex shape of the human heart, different surface and volume based methods have been applied. Major contributions are based on methods as superquadratics, spherical harmonics, or point distribution models (PDM) using minimum description length (MDL) [1–4], as well as methods including physical information [5]. A detailed review of the different approaches is provided in [6]. Except for some recent studies [7–9], all the approaches focus on the left ventricle. These methods succeed in representing the shape of a single object; they differ, however, concerning the effort needed to correlate and analyze shape variations between subjects. All of them are based in some way on manual or automatic landmark setting [5,8, 10,11].

The previous mentioned shape techniques are surface based methods. A different approach is to use the object description via medial skeletons. Those can either be FORMS (=flexible object recognition and modeling system) [12] or the medial representation (m-rep) method, first introduced by Blum [13] and developed later by Pizer [13,14]. The m-rep representation is a multiscale approach, working in a figural

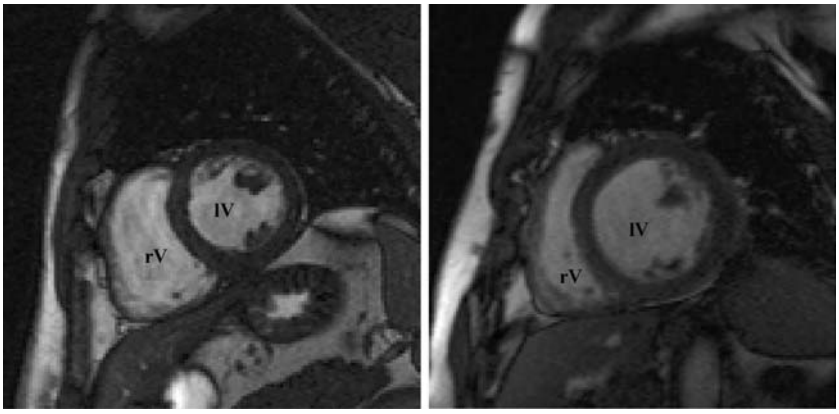

Fig. 1 MRI short axis scan slice of a healthy volunteer (*left*) and a cardiomyopathy patient (*right*) (*IV*: left ventricle, r_V: rogjt vemtroc;e)

coordinate system. It is based on an object hierarchy, and an inner model structure, which implies the outer boundary [14–16]. Furthermore this structure provides correspondence between different subjects for complex multi objects, like the heart, that is not depending on surface landmarks. Up to now several single anatomical objects have already been modeled and analyzed with this method [17]. In a previous study we have already applied this method successfully to a small population of healthy hearts, modeled as an object ensemble and to a cardiac cycle [18,19].

This work focuses on the question, 'if m-reps provide discrimination ability on healthy and diseased hearts?' Figure 1 shows an example MRI slice of a healthy (left side) and diseased heart (right side), suffering from dilatative cardiomyophaty. It has already been shown, that shape differences e.g. in the hippocampus study [20,21] may provide differences between healthy subjects and patients. However, no work has been done on analyzing the shape of the combined cardiac ventricles for a population consisting of healthy and diseased subjects.

Objectives

This work aims at testing the suitability of the m-rep method to model and analyze shape and shape differences between healthy and diseased cardiac ventricles. With this study we want to investigate:

The accuracy of the achieved models for both ventricles.

The ability to discriminate between healthy and diseased hearts.

In the following section, we give a short introduction to the segmentation and modeling technique, and describe the analysis of the model quality with respect to the segmented data. Section 3 provides the statistical results based on 11 healthy and 5 diseased heart data sets. In Sect. Discussion, we conclude with a discussion on the previous mentioned objectives.

Methods

Data

For this experimental study, we use MRI scans of 16 comparable male subjects, 11 healthy volunteers (age: 50 ± 10, mean body surface: $1.94\,m^2$) and 5 diseased patients (age: 57 ± 11, mean body surface: $2.0\,m^2$). The patients suffer from a ventricular dysfunction because of cardiomyopathy (CMP, ejection fraction: $22\pm10\%$) and have been treated either inpatient or ambulantly. The heart geometry is acquired in CINE mode during breath-hold (expiration) using short-axis scans with 5 mm slice thickness and a pixel spacing of 1.56×1.56 mm.

Segmentation

For the level set based segmentation of the heart, we use a software developed at IBIA providing algorithms based on filters of the Insight Segmentation and Registration Toolkit [22,23]. The segmentation process is done on isotropic data with a voxel size of 1.56 mm, using geodesic active contour level sets and shape priors [24]. To get the final binary images (labels) of the two main chambers of the heart, minimal manual refinement is necessary, especially in the region of small anatomical structures (i.e., papillary muscles). Figure 2 shows an example of an original MRI slice including the boundary of the labels (left), and the segmented objects together with the generated boundary of the models (right). The small structures of the papillary muscles are not covered by the model leading to a global shape representation.

Modeling

The concept and application of m-reps has been already described in detail [14,16,25,26]. In brief, the inner structure consists of a grid of atoms along the medial plane of the object and implies the outer boundary, covering the global object shape. This technique has already been applied to a

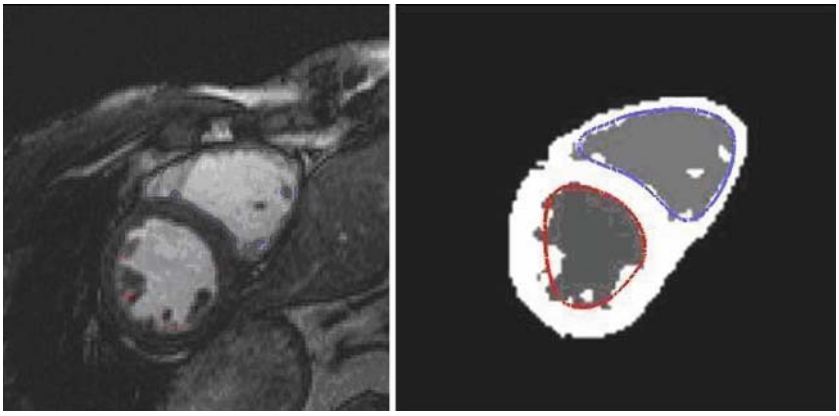

Fig. 2 The original MRI slice and the boundary of the segmented objects (*left*), and the labels together with the generated model boundary (*right*). The model (*solid line*) is not covering details and substructures like the papillary muscles

small population of healthy hearts and one healthy cardiac cycle [19,26]. The m-rep generation is obtained using the semiautomatic optimization technique provided by the software framework "Pablo", developed by the Medical Image and Display Group at the University of North Carolina.

Model quality

One important property of any modeling technique is the ability to correctly represent the modeled objects. To determine the quality of the model to image match we use the similarity index (SI) and the Hausdorff distance (HD).

Similarity index

The SI is calculated using the following formula:

$$S = \frac{2|A \cap B|}{|A| + |B|}, \tag{1}$$

A and B are nonzero pixels in the first and second binary images. Operator |.| represents the size of a set and ∩ represents the intersection of two sets [27].

Hausdorff distance

Since the SI gives a global measure but ignores local extremities, we calculate the HD between the model (A) and the image (B) in terms of non-zero pixels. The undirected HD is computed using

$$H(A, B) = \max\left(h\left(A, B\right), h\left(B, A\right)\right), \tag{2}$$

where

$$h(A, B) = \max_{a \in A} \min_{a \in A} \|a - b\|, \tag{3}$$

is the directed HD.

Mean distance

Integral across the object surface of each vertex distance to the boundary of the binary image object i.e., h(A,B).

Generation of statistical population models

Using a fixed grid of atoms for different subjects allows to establish geometric correspondence by correlating the corresponding atoms. Based on that, PCA can be applied to analyze shape variations. PCA in general has been proven to be useful for understanding geometric variability in populations of parameterized objects e.g., [2]. The statistical framework is well understood when the parameters of objects are elements of an Euclidean vector space. However, shapes which are represented by m-reps operate in a figural space and are not elements of an Euclidean space. Therefore the PCA has been extended by Fletcher et al.[17] to principal geodesic analysis (PGA) which is also valid in figural space.

With this method, we generate a statistical model for the two chambers for all subjects. The output is a model consisting of a mean shape and the principal shape variations.

Results

The models are generated in an iterative way, using a bootstrapping technique. The two ventricles are modeled with the following atom grids: the right ventricle using 20 (4×5) atoms and the left ventricle using 15 (5×3) atoms. The termination of the optimization process is tuned with a threshold that ensures a good global fit (see below) but prevents the m-rep to become irregular following to much into details, like the papillary muscles (see Fig. 2).

Model quality

For all 16 subjects, the global average SI, the average undirected HD, and the average mean Euclidean distance (ED) for the two chambers are summarized in Table 1. The

Table 1 The average similarity index, the Hausdorff distance and the mean Euclidean distance (incl. standard deviation) between the models and labels of all individuals

	Similarity index		Hausdorff distance		Mean euclidean distance	
	IPM	WPM	IPM mm	WPM mm	IPM mm	WPM mm
Left ventricle	0.92±0.01	0.93±0.01	12.38±2.32	4.72±1.29	2.10±0.113	1.91±0.20
Right ventricle	0.90±0.02	0.92±0.03	12.03±4.03	5.14±1.04	2.35±0.264	2.10±0.42

Neglecting the papillary muscles from the calculation leads to the global values. (*IPM*: included papillary muscles; *WPM*: without papillary muscles)

SI is higher than 0.90. The all over mean ED is 2.23 mm and the mean HD is in the range of 12 mm. Excluding the papillary muscles (see Fig. 2) from the calculation leads to higher similarity indices, lower EDs and respectivly better HD, in mean the HD value decreases down to 5 mm.

Model expressiveness

Applying PGA on all 16 subjects, after the m-rep based alignment including scaling, reveals the distribution of shapes shown in Fig. 3. The points 1–11 represent the healthy hearts (blue) and the stars 12–16 represent the diseased hearts (red stars). The first principal component mainly describes the volume ratio between the right and left ventricles. A positive value describes a larger volume of the right ventricle (blue) and a lower volume of the left ventricle (red), a negative value is indicating the opposite. The second principal component describes a thinning and dilation of the right ventricle along the axis through the atrioventricular valve and pulmonary valve. Figure 4 illustrates these two main shape variations: shape for −1 standard deviation (left side), the mean shape (middle), and the +1 standard deviation (right side). The other principal components, higher than two, describe shape variations like elongation, twisting, rotation, bending or combinations, however with less impact to the model.

The first two pc cover more than 40% of the shape space, and the first 10 pc cover about 95% of the shape space.

Discrimination of healthy and diseased hearts

The statistical output allows discrimination in healthy and diseased hearts. The two populations are only separable within the plane of the first two principal components. This small number of healthy and diseased hearts can be separated along a diagonal line through the first two principal components.

Discussion

This paper describes the application of the m-rep method including shape statistics to two different populations (healthy and diseased subjects) for the two main chambers, the left and right ventricle of the heart. It presents first results concerning the achieved model quality and expressiveness.

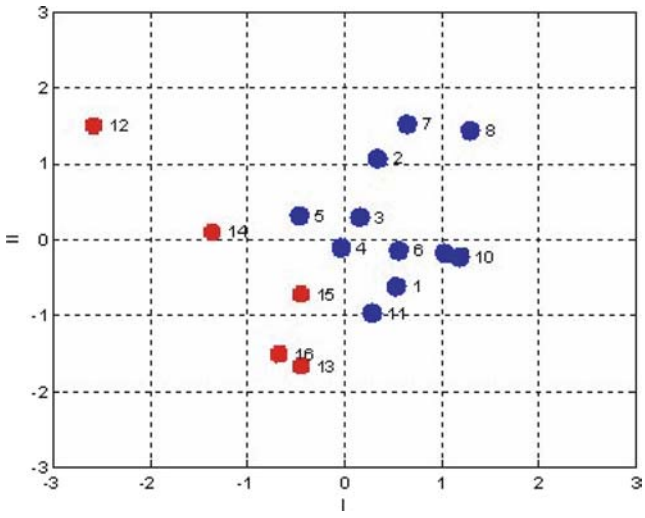

Fig. 3 Principal component distribution of shape changes (I: first main component distribution; II: second main component distribution; *blue dots*: 1–11, healthy hearts; *red stars*: 12–16, diseased hearts)

Model quality

The global analysis of the model to label fit shows a good accuracy within the resolution of the original data. As it can be seen from the SI values (see Table 1) the overall similarity match for both chambers is rather high with values more than 0.9. These values show a very close correspondence between the boundary of the model and the binary image. The HD provides more local distance information and differs among the anatomical structures. For both the ventricles, HD is in the range of 12 mm. These distances are rather high, but they are related to specific anatomical areas within the object (see fig. 2). The high values are detected in the zone of the papillary muscles and in the apex. Excluding the papillary muscles from the HD calculation leads to significantly lower values, decreasing down to HD ∼5 mm. Overall, the mean EDs of ∼2 mm are quite low with respect to the voxel size of 1.56 mm. These quality parameters ensure that the object shapes are covered quite well.

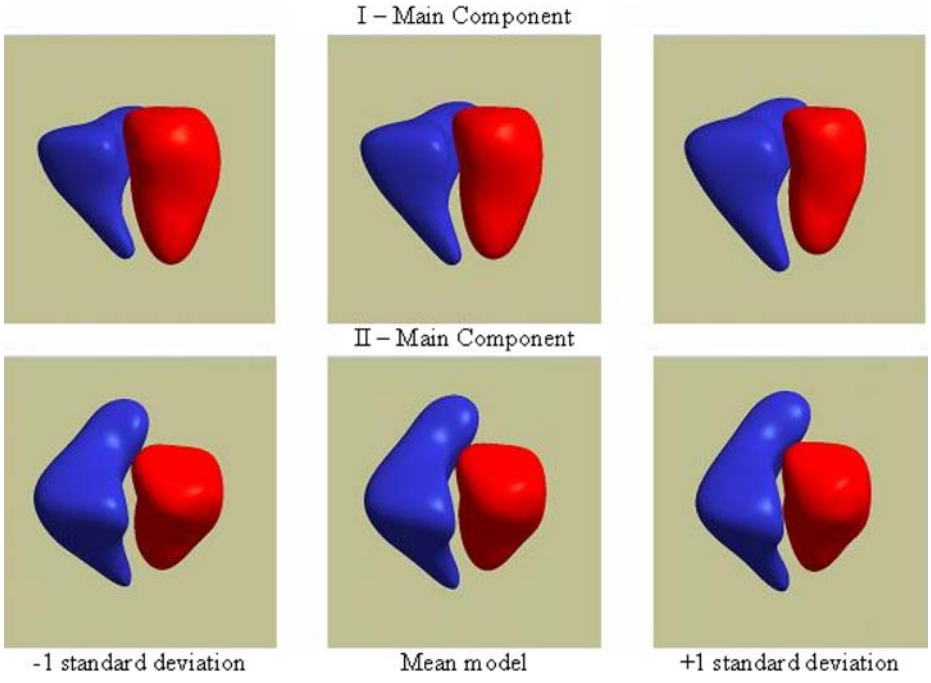

Fig. 4 First (*I*, *frontal view*) and second (*II*, *downward view*) main shape variations: Shape for −1 standard deviation (*left*), the mean shape (*middle*), and the +1 standard deviation (*right*)

The main outcome concerning modeling the ventricles with m-reps is a good global matching: noise and substructures are ignored and any statistical output is global. For making global studies and analysis, as intended in this work, the modelling technique using single m-reps for the ventricles seem to be a good basis. For local studies typical structures like the papillary muscles should be modeled using m-rep subfigures.

It will be a future goal to compare other modeling techniques like PDM using MDL [3,4] or spherical harmonics on this problem.

Model expressiveness

The provided statistics of the object ensemble present a global output of shape differences among healthy and diseased ventricles (see Fig. 3). The common shape model of the heart is given in Fig. 4. The principle modes describe characteristic and meaningful anatomical properties of the population of 16 hearts.

The first principal component especially describes the non linear size ratio of the left and right ventricle. This is physiologically plausible, because of the different volume size of the healthy and diseased hearts, which are characteristic for CMP. The end-diastolic blood volume of the healthy left ventricles is in mean 135 and 230 ml for the diseased ventricles. The volumes of the right ventricles are not significantly different; the volume for the healthy right ventricles is in mean 168 ml, for the diseased ventricles it is 157 ml.

The second mode describes a deformation along the long axis of the heart, especially of the right ventricle. This mode seems to reflect the interdependent shape of the left and right ventricle. Since the volume of the diseased left ventricles increases, the right ventricles have to follow by thinning and surrounding the left ventricle.

Discrimination of healthy and diseased hearts

The most interesting result of this study is that the discrimination between healthy and diseased ventricles is more complex than a volume comparison. The additional variation concerns the deformation of the right ventricle, depending on the deformation of left ventricle. Both principal components cover 40% of the shape space.

Conclusion

The m-rep method, already successfully applied to some less complex topologic anatomical objects, e.g., the kidney and the hippocampus [25], works for the more complicated ventricles of the heart as well.

The high SI (∼0.9 in mean) and the low ED (∼2.2 mm in mean) between the segmented data and the model give a sufficient global shape representation of the individual objects. The decomposition of the complex shape variations is leading to characteristic shape changes, indicating that the two different populations can be discriminated using the first and second principal component. The major result shows the potential of the approach to find additional criterions to the size differences for discrimination. To increase the number of data for healthy and diseased hearts is the crucial point for

the interpretation of the discrimination analysis and is work in progress.

Additionally, future work will have to validate this approach against other modeling techniques, especially the PDM models using MDL [4] in 3D.

Acknowledgements We want to thank the whole Medical Image Display and Analysis Group (MIDAG) from University of North Carolina (Head: Prof. Pizer) for helping in driving problems for m-rep lattice generation. We are further grateful to the members of the whole Institute of Biomedical Image Analysis (IBIA) at the University for Health Sciences, Medical Informatics and Technology (UMIT).

References

1. Bardinet E, Cohen LD, Ayache N (1996) Tracking and motion analysis of the left ventricle with deformable superquadrics. Med Image Anal 1:129–149
2. Cootes TF, Taylor CJ, Hill A, Haslam J (1993) The Use of Active Shape Models for locating Structures. Presented at 13′th international conference on information processing in medical imaging
3. Cootes TF, Taylor CJ, Cooper DH, Graham J (1995) Active shape models: their training and applications. Comput Vis Image Underst 61:38–59
4. Davies RH, Twining CJ, Cootes TF, Waterton JC, Taylor CJ (2002) A minimum description length approach to statistical shape modeling. IEEE Trans Med Imaging 21:525–537
5. Wang Y, Staib LH (2000) Physical model-based non-rigid registration incorporating statistical shape information. Med Image Anal 4:7–20
6. Frangi AF, Niessen WJ, Viergever MA (2001) Three-dimensional modeling for functional analysis of cardiac images: a review. IEEE Trans Med Imaging 20:2–25
7. Mitchell SC, Lelieveldt BP, van der Geest RJ, Bosch HG, Reiber JH, and M. Sonka (2001) Multistage hybrid active appearance model matching: segmentation of left and right ventricles in cardiac MR images. IEEE Trans Med Imaging 20:415–423
8. Frangi AF, Rueckert D, Schnabel JA, Niessen WJ (2002) Automatic construction of multiple-object three-dimensional statistical shape models: application to cardiac modeling. IEEE Trans Med Imaging 21:1151–1166
9. Lotjonen J, Kivisto S, Koikkalainen J, Smutek D, Lauerma K (2004) Statistical shape model of atria, ventricles and epicardium from short- and long-axis MR images. Med Image Anal 8: 371–386
10. Brett AD, Taylor CJ (2000) A method of automated landmark generation for automated 3D PDM construction. Image Vis Comput 18:739–748
11. Brett AD, Taylor CJ (2000) Construction of 3D shape models of femoral articular cartilage using harmonic maps. Presented at MICCAI
12. Zhu SC, Yuille AL (1996) Forms: a flexible object recognition and modeling system. Int J Comput Vis 20:187–212
13. Blum H (1967) A transformation for extracting new descriptors of shape. In: Models for the perception of speech and visual Form, Wathen-Dunn W (ed). MIT Press, Cambridge, pp 363–380
14. Pizer SM, Fritsch DS, Yushkevich PA, Johnson VE, Chaney EL (1999) Segmentation, registration, and measurement of shape variation via image object shape. IEEE Trans Med Imaging 18: 851–865
15. Pizer SM (2003) Guest editoral-medial and medical: a good match for image analysis. Int J Comput Vis 55:79–84
16. Joshi S, Pizer S, Fletcher PT, Yushkevich P, Thall A, Marron JS (2002) Multiscale deformable model segmentation and statistical shape analysis using medial descriptions. IEEE Trans Med Imaging 21:538–550
17. Fletcher PT, Joshi S, Lu C, Pizer S (2003) Gaussian distributions on Lie groups and their application to statistical shape analysis. Inf Process Med Imaging 18:450–462
18. Pilgram R, Fritscher KD, Fletcher PT, Schubert R (2004) Shape modeling of the multiobject organ heart. Presented at BioMED, Innsbruck
19. Pilgram R, Fritscher KD, Schubert R (2004) Modeling of the geometric variation and analysis of the right atrium and right ventricle motion of the human heart using PCA. Presented at CARS, Chicago
20. Styner M (2003) Automatic and robust computation of 3D medial models incorporating object variability. Int J Comput Vis 55: 107–122
21. Golland P, Grimson W, Shenton M, Kikinis R (2005) Detection and analysis of statistical differences in anatomical shape. Med Image Anal 9:69–86
22. NLM Insight Segmentation and Registration Toolkit
23. Fritscher KD, Schubert R (2005) A software framework for preprocessing and level-set segmentation of medical data. Presented at SPIE medical imaging, San Diego
24. Leventon M, Grimson W, Faugeras O (2000) Statistical Shape Influence in Geodesic Active Contours. Comput Vis Pattern Recognit 1:316–323
25. Pizer SM, Fletcher PT, Joshi S, Thall A, Chen JZ, Fridman Y, Fritsch DS, Gash G, Glotzer JM, Jiroutek MR, Lu C, Muller KE, Tracton G, Yushkevich PA, Chaney EL (2003) Deformable m-reps for 3D medical image segmentation. Int J Comput Vis 55(2/3): 85–106
26. Pilgram R, Fritscher K, Fletcher PT, Schubert R (2004) Shape Modeling of the multiobject organ heart. Presented at BioMED, Innsbruck
27. Zijdenbos AP, Dawant BM, Margolin RA, Palmer AC (1994) Morphometric analysis of white matter lesions in MR images: method and validation. IEEE Trans Med Imaging 13:716–724